

WEIGHTED AND MULTI-TASK LOSS FOR RARE AUDIO EVENT DETECTION

Huy Phan*, Martin Krawczyk-Becker†, Timo Gerkmann‡, and Alfred Mertins‡

* University of Oxford, Department of Engineering Science, Oxford, UK

† University of Hamburg, Department of Informatics, Hamburg, Germany

‡ University of Lübeck, Institute for Signal Processing, Lübeck, Germany

huy.phan@eng.ox.ac.uk, {krawczyk,gerkmann}@informatik.uni-hamburg.de,

mertins@isip.uni-luebeck.de

ABSTRACT

We present in this paper two loss functions tailored for rare audio event detection in audio streams. The weighted loss is designed to tackle the common issue of imbalanced data in background/foreground classification while the multi-task loss enables the networks to simultaneously model the class distribution and the temporal structures of the target events for recognition. We study the proposed loss functions with deep neural networks (DNNs) and convolutional neural networks (CNNs) coupled with state-of-the-art phase-aware signal enhancement. Experiments on the DCASE 2017 challenge’s data show that our system with the proposed losses significantly outperforms not only the DCASE 2017 baseline but also our baseline which has a similar network architecture and a standard loss function.

Index Terms— audio event detection, convolutional neural networks, deep neural networks, weighted loss, multi-task loss

1. INTRODUCTION

There is an ongoing methodological trend in computational auditory scene analysis, shifting from conventional methods to modern deep learning techniques [1, 2, 3, 4, 5, 6]. However, most of the works have focused on the aspect of network architectures which have been usually adapted from those successful in related fields, such as computer vision and speech recognition. Little attention has been paid to loss functions of the networks. Although the common loss functions, such as the cross-entropy loss for classification and the ℓ_2 -distance loss for regression, work for general settings, it is arguable that the loss functions should be tailored for a particular task at hand.

In this work, we propose two such tailored loss functions, namely *weighted loss* and *multi-task loss* to tackle the well-known issues of rare audio event detection (RAED). The weighted loss can be used to explicitly weight penalties for two types of errors (i.e. false negative and false positive errors) in a binary classification problem. This loss is, therefore, useful for imbalanced background/foreground classification in RAED in which the foreground samples are more valuable than the numerous background samples and should be penalized stronger if misclassified. The multi-task loss is proposed to suit the classification of target events. As audio events possess inherent temporal structures, modelling them has been shown important for recognition [7, 8, 9] and detection [10, 11]. The multi-task loss is designed to allow a network to model both event class distribution (as a classification task) and event temporal structures (as a regression task for event onset and

offset estimation) at the same time. By doing this, the network is forced to cope with a more complex problem rather than the simple classification one. As a result, the network is implicitly regularized, leading to improvements of its generalization capability.

In this work, we study the coupling of the proposed loss functions with both DNNs and CNNs for rare audio event detection. Experimental results conducted on the development and evaluation data of the DCASE 2017 challenge show that the proposed system significantly outperforms the challenge’s baseline system. Furthermore, compared to our baseline, which is similar to the proposed system except for the loss function, significant improvements can also be seen.

2. THE PROPOSED DETECTION SYSTEM

The overall pipeline of the proposed detection system is illustrated in Fig. 1. The audio signals are firstly preprocessed for signal enhancement (cf. Section 2.1). The preprocessed signals are then decomposed into small frames and frame-wise feature extraction is performed. The proposed systems accomplish the detection goal in two steps: background rejection and event classification. The former uses a binary classifier to filter out background frames and lets only foreground frames go through. Subsequently, the latter employs a multi-class classifier to distinguish the frames identified as foreground into three target categories. We investigate both DNNs and CNNs for classification. The networks for background/foreground and event classification have similar body architecture while their output layers and loss functions are task-dependant as illustrated in Fig. 2.

2.1. Phase-aware signal enhancement

For all three categories, baby cry, glass break, and gun shot, short-time discrete Fourier transform (STFT) domain signal enhancement was employed to reduce acoustic noise in the recordings. The STFT segments had a length of 32 ms with consecutive segments overlapping by 50 %. For analysis and synthesis, a square-root Hann window was used. The STFT magnitudes of the clean signals were estimated from the noisy signals according to [12], with its parameters set to $\mu^{[12]} = \beta^{[12]} = 0.5$, and combined with the noisy phase for the reconstruction of the enhanced time domain signal. The magnitude estimation in [12] relies on the power spectral densities (PSDs) of noise and speech as well as estimates of the clean STFT phase. The speech PSD was estimated via [13] and the noise PSD via temporal cepstrum smoothing [14, 15]. Estimates of the clean STFT phase were obtained according to [16], which in turn relies on estimates of the fundamental frequency of the desired sound.

*The work was performed when H. Phan was at the Institute of Signal Processing, University of Lübeck.



Fig. 1. The overall pipeline of the proposed audio event detection system.

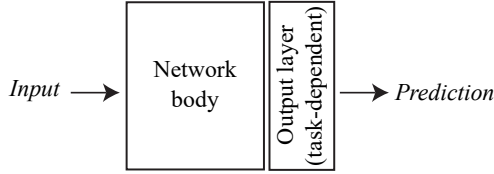


Fig. 2. The abstract network architecture.

Accordingly, [16] provides estimates of the clean phase only for sounds for which a fundamental frequency is defined, i.e. harmonic sounds such as baby cries. Harmonic sounds and their fundamental frequency were found using the noise robust fundamental frequency estimator PEFAC [17]. To focus on baby cries, we limited the search range of PEFAC to frequencies between 300 Hz and 750 Hz, which covers the relatively high fundamental frequency of most baby cries while excluding lower frequencies that are found in adult speech. As proposed in [12], for all non-voiced sounds we employed the phase-blind spectral magnitude estimator [18], which does not need any clean phase estimate.

Finally, to avoid undesired distortions of the desired signal, we limited the maximum attenuation that can be applied to each STFT time-frequency point to 12 dB.

2.2. DNNs

As previously mentioned, the DNNs for background/foreground and event classification share a similar body architecture, which is described in Table 1. The only difference is the dropout probability which was set to 0.5 for the former and 0.2 for the latter.

Regarding the network input, an audio signal was decomposed into frames of length 100 ms with a hop size of 20 ms. 64 log Gammatone spectral coefficients [19] in the frequency range of 50 Hz to 22050 Hz were then extracted for each frame. In addition, we considered a context of five frames for classification purpose. The feature vector for a context window was formed by simply concatenating feature vectors of its five constituent frames.

2.3. CNNs

The network body architecture of the CNNs are elaborated in Table 2. For background/foreground classification, the number of feature maps of each convolutional layer was set to 64 and the dropout probability was set to 0.5. Those for event classification were 128 and 0.2, respectively.

The CNNs receive a log Gammatone spectral image as input. An audio signal was decomposed into frames of length 40 ms with a hop size of 20 ms. A feature set of 64 log Gammatone spectral coefficients was then calculated for each frame as in the DNN case. In addition, delta and acceleration coefficients were also calculated using a window length of nine frames. Eventually, 64 consecutive frames were combined into a $64 \times 64 \times 3$ image which was used as input for the CNNs.

2.4. Weighted loss for foreground/background classification

In general, for audio event detection in continuous streams, the number of background frames is significantly larger than for foreground ones. This leads to a skewed classification problem with a dominance of the background samples. The skewness is even more severe

Table 1. The parameters of the DNN architecture. A dropout probability of 0.5 and 0.2 is used for background rejection and event classification, respectively.

Layer	Size	Activation	Dropout
fc1	512	ReLU	0.5/0.2
fc2	256	ReLU	0.5/0.2
fc3	512	ReLU	0.5/0.2

in case of the RAED task. To remedy this skewness issue, in combination with data resampling, we propose a *weighted loss* function to train the networks.

Firstly, the background samples were downsampled by a factor of 5. Furthermore, the set of foreground samples was upsampled by an integer factor to make its size approximately equal to the background set. Let us denote a training set of N training examples as $\{(\mathbf{x}_1, \mathbf{y}_1), \dots, (\mathbf{x}_N, \mathbf{y}_N)\}$ where \mathbf{x} denotes a one-dimensional feature vector (in case of DNN) or a three-dimensional image (in case of CNN). $\mathbf{y} \in \{0, 1\}^C$ denotes a binary one-hot encoding vector with $C = 2$ in this case.

Typically, for a classification task, a network will be trained to minimize the cross-entropy loss

$$E(\boldsymbol{\theta}) = -\frac{1}{N} \sum_{n=1}^N \mathbf{y}_n \log(\hat{\mathbf{y}}_n(\mathbf{x}_n, \boldsymbol{\theta})) + \frac{\lambda}{2} \|\boldsymbol{\theta}\|_2^2, \quad (1)$$

where $\boldsymbol{\theta}$ denotes the network’s trainable parameters and the hyper-parameter λ is used to trade-off the error term and the ℓ_2 -norm regularization term. The predicted posterior probability $\hat{\mathbf{y}}(\mathbf{x}, \boldsymbol{\theta})$ is obtained by applying the softmax function on the network output layer. However, this loss penalizes different classification errors equally. In contrast, our proposed weighted loss, described below, enables us to penalize individual classification errors differently. The weighted loss reads

$$E_w(\boldsymbol{\theta}) = -\frac{1}{N} \left(\lambda_{\text{fg}} \sum_{n=1}^N \mathbb{I}_{\text{fg}}(\mathbf{x}_n) \mathbf{y}_n \log(\hat{\mathbf{y}}_n(\mathbf{x}_n, \boldsymbol{\theta})) + \lambda_{\text{bg}} \sum_{n=1}^N \mathbb{I}_{\text{bg}}(\mathbf{x}_n) \mathbf{y}_n \log(\hat{\mathbf{y}}_n(\mathbf{x}_n, \boldsymbol{\theta})) \right) + \frac{\lambda}{2} \|\boldsymbol{\theta}\|_2^2, \quad (2)$$

where $\mathbb{I}_{\text{fg}}(\mathbf{x})$ and $\mathbb{I}_{\text{bg}}(\mathbf{x})$ are indicator functions which specify whether the sample \mathbf{x} is foreground or background, respectively. λ_{fg} and λ_{bg} are *penalization weights* for false negative errors (i.e. a foreground sample is misclassified as background) and false positive errors (i.e. a background sample is misclassified as foreground), respectively. Since foreground samples are more valuable than background ones in the skewed classification problem at hand, we penalize false negative errors more than false positive ones (cf. Section 3.2).

2.5. Multi-task loss for event classification

Beyond a simple event classification, we enforce the networks to jointly model the class distribution for event classification and the event temporal structures for onset and offset distance estimation similar to [20]. The proposed *multi-task loss* is specialized for this

Table 2. The parameters of the CNN architecture. The number of feature maps and the dropout probability are set to 64 and 0.5, respectively, for background rejection while they are set to 128 and 0.2, respectively, for event classification.

Layer	Size	#Fmap	Activation	Dropout
conv1	3 × 3	64/128	ReLU	-
conv2	3 × 3	64/128	ReLU	-
maxpool2	2 × 1	-	-	0.5/0.2
conv3	3 × 3	64/128	ReLU	-
conv4	3 × 3	64/128	ReLU	-
maxpool4	2 × 2	-	-	0.5/0.2
fc1	1024	-	ReLU	0.5/0.2
fc2	1024	-	ReLU	0.5/0.2

Output layer

Prediction

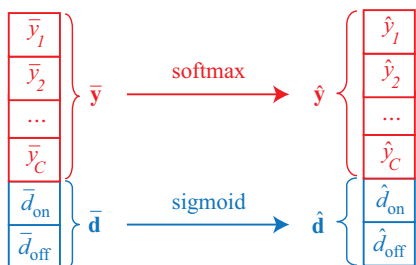


Fig. 3. The output layer and the prediction of a multi-task network (i.e. a DNN or a CNN).

purpose. Multi-task modeling can be interpreted as implicit regularization which is expected to improve generalization of a network [21, 22].

In addition to the one-hot encoding vector $\mathbf{y} \in \{0, 1\}^C$ (C is the number of target event categories in this case), we associated a sample \mathbf{x} with a distance vector $\mathbf{d} = (d_{\text{on}}, d_{\text{off}}) \in \mathbb{R}^2$. d_{on} and d_{off} denote the distances from the center frame of \mathbf{x} to the corresponding event onset and offset [10, 23]. The onset and offset distances were normalized to $[0, 1]$ by dividing by their maximum values.

The output layer of a multi-task network (i.e. a DNN or a CNN) consists of two variables: $\bar{\mathbf{y}} = (\bar{y}_1, \bar{y}_2, \dots, \bar{y}_C)$ and $\bar{\mathbf{d}} = (\bar{d}_{\text{on}}, \bar{d}_{\text{off}})$ as illustrated in Fig. 3. The network predictions for class posterior probability $\hat{\mathbf{y}} = (\hat{y}_1, \hat{y}_2, \dots, \hat{y}_C)$ and distance vector $\hat{\mathbf{d}} = (\hat{d}_{\text{on}}, \hat{d}_{\text{off}})$ are then obtained by:

$$\hat{\mathbf{y}} = \text{softmax}(\bar{\mathbf{y}}), \quad (3)$$

$$\hat{\mathbf{d}} = \text{sigmoid}(\bar{\mathbf{d}}). \quad (4)$$

Given a training set $\{(\mathbf{x}_1, \mathbf{y}_1, \mathbf{d}_1), \dots, (\mathbf{x}_N, \mathbf{y}_N, \mathbf{d}_N)\}$ of N samples, the network is trained to minimize the following *multi-task loss* function:

$$E_{\text{mt}}(\boldsymbol{\theta}) = \lambda_{\text{class}} E_{\text{class}}(\boldsymbol{\theta}) + \lambda_{\text{dist}} E_{\text{dist}}(\boldsymbol{\theta}) + \lambda_{\text{conf}} E_{\text{conf}}(\boldsymbol{\theta}) + \frac{\lambda}{2} \|\boldsymbol{\theta}\|_2^2, \quad (5)$$

where

$$E_{\text{class}}(\boldsymbol{\theta}) = -\frac{1}{N} \sum_{n=1}^N \mathbf{y}_n \log(\hat{\mathbf{y}}_n(\mathbf{x}_n, \boldsymbol{\theta})), \quad (6)$$

$$E_{\text{dist}}(\boldsymbol{\theta}) = -\frac{1}{N} \sum_{n=1}^N \left\| \mathbf{d} - \hat{\mathbf{d}}_n(\mathbf{x}_n, \boldsymbol{\theta}) \right\|_2^2, \quad (7)$$

$$E_{\text{conf}}(\boldsymbol{\theta}) = -\frac{1}{N} \sum_{n=1}^N \left\| \mathbf{y}_n - \hat{\mathbf{y}}_n \frac{I(\mathbf{d}_n, \hat{\mathbf{d}}_n(\mathbf{x}_n, \boldsymbol{\theta}))}{U(\mathbf{d}_n, \hat{\mathbf{d}}_n(\mathbf{x}_n, \boldsymbol{\theta}))} \right\|_2^2. \quad (8)$$

$E_{\text{class}}(\boldsymbol{\theta})$, $E_{\text{class}}(\boldsymbol{\theta})$, and $E_{\text{conf}}(\boldsymbol{\theta})$ in above equations are so-called *class loss*, *distance loss*, and *confidence loss*, respectively. The terms λ_{class} , λ_{dist} , and λ_{conf} represent the weighting coefficients for three corresponding loss types. The *class loss* complies with the common cross-entropy loss to penalize classification errors whereas the *distance loss* penalizes event onset and offset distance estimation errors. Furthermore, the *confidence loss* penalizes both classification errors and distance estimation errors. The functions $I(\mathbf{d}, \hat{\mathbf{d}})$ and $U(\mathbf{d}, \hat{\mathbf{d}})$ in (8) calculate the intersection and the union of the ground-truth event boundary and the predicted one, given by:

$$I(\mathbf{d}, \hat{\mathbf{d}}) = \min(d_{\text{on}}, \hat{d}_{\text{on}}) + \min(d_{\text{off}}, \hat{d}_{\text{off}}), \quad (9)$$

$$U(\mathbf{d}, \hat{\mathbf{d}}) = \max(d_{\text{on}}, \hat{d}_{\text{on}}) + \max(d_{\text{off}}, \hat{d}_{\text{off}}). \quad (10)$$

While the network may favor to optimize the class loss or the distance loss to reduce the total loss $E_{\text{mt}}(\boldsymbol{\theta})$, the confidence loss encourages it to optimize both losses at the same time. This is expected to accelerate and facilitate the learning process.

2.6. Inference

We opted for a simple inference scheme here for target event segmentation. Firstly, we performed thresholding on the posterior probability output by the background-rejection classifier. A sample classified with a foreground posterior probability above a threshold α_{prob} will be subsequently forwarded to the event classifier to determine the event class label. Afterwards, an output label sequence was then smoothed by a median filter with a window length w_{sm} .

Note that we did not use the estimates for event onset and offset distances provided by the event classification network. This can be further explored in future work as in [10, 23].

3. EXPERIMENTS

3.1. DCASE 2017 data

We conducted experiments on the data of ‘‘Detection of rare events’’ task of the DCASE 2017 challenge [24]. This data includes two sets: development and evaluation data. For the former, isolated events of three target categories (i.e. *baby cry*, *glass break*, and *gunshot*) downloaded from freesound.org were mixed with background recordings from TUT Acoustic Scenes 2016 development dataset [25] with an event presence rate of 0.5 to create 500 mixtures for each category in both training and testing subsets. The mixing event-to-background ratios (EBR) were -6, 0 and 6 dB. The development data was published during the challenge. The evaluation data was created in a similar manner with 500 mixtures for each category and was kept private during the challenge.

3.2. Parameters

For the weighted loss in (2), we set $\lambda_{\text{fg}} = 10$ and $\lambda_{\text{bg}} = 1$. That is, false negatives were penalized ten times more than false positives. The associated weights of the multi-task loss in (5) were set to $\lambda_{\text{class}} = 1$, $\lambda_{\text{dist}} = 10$, and $\lambda_{\text{conf}} = 1$. We set λ_{dist} larger than λ_{class} and λ_{conf} to encourage the networks to focus more on modeling event temporal structures. In addition, we set the regularization parameter $\lambda = 10^{-3}$ for both losses. The networks were trained using the *Adam* optimizer [26] with a learning rate of 10^{-4} . The

Table 3. Event-based performance the development data.

	DCASE baseline		Our baseline						Proposed system					
			DNN		CNN		Best combination		DNN		CNN		Best combination	
	ER	F1	ER	F1	ER	F1	ER	F1	ER	F1	ER	F1	ER	F1
Baby cry	0.67	72.0	0.38	80.3	0.11	94.7	0.11	94.7	0.36	80.5	0.09	95.3	0.09	95.3
Glass break	0.22	88.5	0.08	96.2	0.15	92.5	0.08	96.2	0.10	95.3	0.20	89.5	0.10	95.3
Gun shot	0.69	57.4	0.32	82.1	0.35	80.6	0.32	82.1	0.36	79.5	0.38	79.1	0.36	79.5
Average	0.53	72.7	0.26	86.2	0.20	89.3	0.17	91.0	0.27	85.1	0.22	88.0	0.18	90.0

Table 4. Event-based performance the evaluation data.

	DCASE baseline		Our baseline		Proposed system	
	ER	F1	ER	F1	ER	F1
Baby cry	0.80	66.8	0.28	85.6	0.23	88.4
Glass break	0.38	79.1	0.16	91.6	0.11	94.3
Gun shot	0.73	46.5	0.33	80.7	0.32	82.1
Average	0.64	64.1	0.26	86.1	0.22	88.2

DNNs were trained for 200 epochs with a batch size of 256 whereas the CNNs were trained for 5 epochs with a batch size of 128.

Note that although Task 2 of the challenge is set up to evaluate detection of target event categories separately, our proposed system is multi-class, aiming at detecting all the three target categories at once. By doing this, we avoid optimizing different systems for individual categories.

3.3. Evaluation metrics and baseline systems

We used two event-based metrics for evaluation: detection error (ER) and F-score [27] as used for the challenge. We compared the detection performances obtained by our proposed system to that of the DCASE 2017 baseline [24]. This baseline uses log mel-band energies as features and consists of class-specific 2-layer DNNs followed by median filtering for post-processing. In addition to the DCASE baseline, to investigate effects of the proposed loss functions, we also developed our baseline which is similar to the proposed system except that the standard cross-entropy loss was used.

3.4. Experimental results on the development data

In the inference step of the experiment on the development data, the probability threshold α_{prob} was searched in the range of [0, 1] with a step size of 0.05. In addition, we performed grid search for the smoothing window length w_{sm} for each category in the range of [3, 147] with a step size of 6. The values of α_{prob} and w_{sm} yielding the best F-score were retained.

The detection performances on the development data are shown in Table 3. As can be seen from our proposed as well as our baseline systems, the performances of the proposed DNN and CNN detectors vary significantly for different event categories. While the former is more efficient in detecting glass break and gun shot events, the latter performs better on human-generated baby cry events. It seems that invariant features learned by a CNN, which are capable of handling the well-known vocal-tract length variation between speakers in speech recognition [28, 29, 30], are helpful for baby cry. In contrast, convolution does not help but worsens the detection performance of the non-human events (i.e. glass break and gun shot). Probably, these events do not possess the characteristics as human-generated events, and information in neighboring frequency bands should not be pooled. As a result, the DNN detector works better for these events than the CNN one, at least in our setup.

Both our proposed and baseline systems, either individual DNN or CNN detectors or their best combination, outperform the DCASE baseline over all categories with a large margin. In addition, our proposed and baseline perform comparably. However, their results on the development data are subject to overfitting and should not be used for justification since the inference parameters (i.e. the probability threshold and the smoothing window) were searched to maximize the performance on the known test set of the development data.

3.5. Experimental results on the evaluation data

The settings of our proposed and baseline systems on the private-held evaluation data are based on the best combination found in the experiment with the development data. That is, the CNN is in charge of detecting baby cry events while the DNN is responsible for detecting glass break and gun shot events. In combination with state-of-the-art phase-aware signal enhancement, the parameters that led to the best performance on the development data were retained, except for the smoothing window size w_{sm} . We experimentally saw a strong influence of this parameter on the detection performance of the development data. Therefore, we chose the one that produced an event presence rate nearest to 0.5 which is the value used for generating the data [24]. The whole development data was used for training in this experiment.

The results on the evaluation data are shown in Table 4. The proposed system with the tailored loss achieves an F-score of 88.2% and an ER of 0.22 which are significantly better than those obtained by the DCASE baseline. Moreover, the tailored-loss system also outperforms our baseline based on the standard cross-entropy loss, improving 2.1% absolute on F-score and reducing 0.04 absolute on ER. Improvements on individual categories can also be seen.

Participating in the DCASE 2017 challenge, our team is ranked 3rd out of 13 participating teams [31]. Note that the results of the proposed system in Table 4 were obtained after correcting a minor mistake in our submission system [32]. Therefore, they are slightly different from those in the official DCASE webpage [31], thanks to the organization team for their support in unofficial evaluation. Last but not least, although we have only studied with common DNN and CNN architectures, the proposed loss functions can be used for other network architectures in replacement of the standard loss function.

4. CONCLUSIONS

We proposed two tailored loss functions to couple with DNNs and CNNs to address the common issues of rare audio event detection problem. The weighted loss is designed to tackle the data skewness issue in background/foreground classification and the multi-task loss enables the networks to jointly model event class distribution and event temporal structures for event classification. In combination with state-of-the-art phase-aware signal enhancement, we reported significant improvements in detection performance on the DCASE 2017 challenge data obtained by our proposed system over the challenge’s baseline as well as our own baseline.

5. REFERENCES

- [1] I. McLoughlin, H. Zhang, Z. Xie, Y. Song, and W. Xiao, "Robust sound event classification using deep neural networks," *IEEE/ACM Trans. on Audio, Speech, and Language Processing*, vol. 23, no. 3, pp. 540–552, 2015.
- [2] I. McLoughlin, H. Zhang, Z. Xie, Y. Song, W. Xiao, and H. Phan, "Continuous robust sound event classification using time-frequency features and deep learning," *PLoS ONE*, vol. 12, no. 9, 2017.
- [3] N. Takahashi, M. G. and B. Pfister, and L. V. Gool, "Deep convolutional neural networks and data augmentation for acoustic event recognition," in *Proc. INTERSPEECH*, 2016, pp. 2982–2986.
- [4] A. Kumar and B. Raj, "Deep cnn framework for audio event recognition using weakly labeled web data," *arXiv:1707.02530*, 2017.
- [5] E. Çakir, G. Parascandolo, T. Heittola, H. Huttunen, and T. Virtanen, "Convolutional recurrent neural networks for polyphonic sound event detection," *IEEE/ACM Trans. on Audio, Speech, and Language Processing (TASLP)*, vol. 5, no. 6, pp. 1291–1303, 2017.
- [6] H. Phan, L. Hertel, M. Maass, and A. Mertins, "Robust audio event recognition with 1-max pooling convolutional neural networks," in *Proc. Interspeech*, 2016, pp. 3653–3657.
- [7] J. Dennis, Y. Qiang, T. Huajin, T. H. Dat, and L. Haizhou, "Temporal coding of local spectrogram features for robust sound recognition," in *Proc. ICASSP*, 2013, pp. 803–807.
- [8] A. Kumar, P. Dighe, R. Singh, S. Chaudhuri, and B. Raj, "Audio event detection from acoustic unit occurrence patterns," in *Proc. ICASSP*, 2012, pp. 489–492.
- [9] H. Phan, M. Maass, L. Hertel, R. Mazur, I. McLoughlin, and A. Mertins, "Learning compact structural representations for audio events using regressor banks," in *Proc. ICASSP*, 2016, pp. 211–215.
- [10] H. Phan, M. Maaß, R. Mazur, and A. Mertins, "Random regression forests for acoustic event detection and classification," *IEEE/ACM Trans. on Audio, Speech, and Language Processing*, vol. 23, no. 1, pp. 20–31, 2015.
- [11] G. Parascandolo, H. Huttunen, and T. Virtanen, "Recurrent neural networks for polyphonic sound event detection in real life recordings," in *Proc. ICASSP*, 2016, pp. 6440–6444.
- [12] T. Gerkmann and M. Krawczyk, "MMSE-optimal spectral amplitude estimation given the STFT-phase," *IEEE Signal Process. Lett.*, vol. 20, no. 2, pp. 129–132, Feb. 2013.
- [13] T. Gerkmann and R. C. Hendriks, "Unbiased MMSE-based noise power estimation with low complexity and low tracking delay," *IEEE Trans. Audio, Speech, Language Process.*, vol. 20, no. 4, pp. 1383–1393, May 2012.
- [14] C. Breithaupt, T. Gerkmann, and R. Martin, "A novel a priori SNR estimation approach based on selective cepstro-temporal smoothing," in *IEEE Int. Conf. Acoust., Speech, Signal Process. (ICASSP)*, Las Vegas, NV, USA, Apr. 2008, pp. 4897–4900.
- [15] T. Gerkmann and R. Martin, "On the statistics of spectral amplitudes after variance reduction by temporal cepstrum smoothing and cepstral nulling," *IEEE Trans. Signal Process.*, vol. 57, no. 11, pp. 4165–4174, Nov. 2009.
- [16] M. Krawczyk and T. Gerkmann, "STFT phase reconstruction in voiced speech for an improved single-channel speech enhancement," *IEEE/ACM Trans. Audio, Speech, Language Process.*, vol. 22, no. 12, pp. 1931–1940, Dec 2014.
- [17] S. Gonzalez and M. Brookes, "PEFAC – a pitch estimation algorithm robust to high levels of noise," *IEEE Trans. Audio, Speech, Language Process.*, vol. 22, no. 2, pp. 518–530, Feb. 2014.
- [18] C. Breithaupt, M. Krawczyk, and R. Martin, "Parameterized MMSE spectral magnitude estimation for the enhancement of noisy speech," in *IEEE Int. Conf. Acoust., Speech, Signal Process. (ICASSP)*, Las Vegas, NV, USA, Apr. 2008, pp. 4037–4040.
- [19] D. P. W. Ellis. (2009) Gammatone-like spectrograms. [Online]. Available: <http://www.ee.columbia.edu/~dpwe/resources/matlab/gammatonegram/>
- [20] H. Phan, L. Hertel, M. Maass, P. Koch, and A. Mertins, "CaR-Forest: Joint classification-regression decision forests for overlapping audio event detection," *arXiv:1607.02306*, 2016.
- [21] J. Redmon, S. K. Divvala, R. B. Girshick, and A. Farhadi, "You only look once: Unified, real-time object detection," in *Proc. CVPR*, 2016, pp. 779–788.
- [22] S. Ruder, "An overview of multi-task learning in deep neural networks," *arXiv:1706.05098*, 2017.
- [23] H. Phan, M. Maass, R. Mazur, and A. Mertins, "Early event detection in audio streams," in *Proc. ICME*, 2015, pp. 1–6.
- [24] A. Mesaros, T. Heittola, A. Diment, B. Elizalde, A. Shah, E. Vincent, B. Raj, and T. Virtanen, "DCASE 2017 challenge setup: tasks, datasets and baseline system," in *Proc. the Detection and Classification of Acoustic Scenes and Events 2017 Workshop (DCASE2017)*, 2017.
- [25] A. Mesaros, T. Heittola, and T. Virtanen, "TUT database for acoustic scene classification and sound event detection," in *Proc. EUSIPCO*, 2016.
- [26] D. P. Kingma and J. L. Ba, "Adam: a method for stochastic optimization," in *Proc. ICLR*, 2015, pp. 1–13.
- [27] A. Mesaros, T. Heittola, and T. Virtanen, "Metrics for polyphonic sound event detection," *Applied Sciences*, vol. 6, no. 6, 2016.
- [28] A. Mertins and J. Rademacher, "Vocal tract length invariant features for automatic speech recognition," in *Proc. Automatic Speech Recognition and Understanding Workshop (ASRU)*, 2005, pp. 308–312.
- [29] N. Jaitly and G. E. Hinton, "Vocal tract length perturbation (vtlp) improves speech recognition," in *Proc. ICML 2013 Workshop on Deep Learning for Audio, Speech and Language Processing*, 2013.
- [30] X. Cui, V. Goel, and B. Kingsbury, "Data augmentation for deep neural network acoustic modeling," *IEEE/ACM Trans. on Audio, Speech and Language Processing (TASLP)*, vol. 23, no. 9, pp. 1469–1477, 2015.
- [31] <http://www.cs.tut.fi/sgn/arg/dcase2017/>.
- [32] H. Phan, M. Krawczyk-Becker, T. Gerkmann, and A. Mertins, "DNN and CNN with weighted and multi-task loss functions for audio event detection," *arXiv:1708.03211*, 2017.